

# Implementation of SEPIC/Zeta Three-Port Bidirectional DC-DC Converter for Renewable Energy Applications

Venmathi M, Ramaprabha R

Department of Electrical and Electronics Engineering, SSN College of Engineering, India

**Abstract-** In this paper an efficient topology of (Single Ended Primary Inductor Converter) SEPIC/Zeta converter is proposed to interface renewable energy sources and the load. The proposed converter is obtained by the integration of the bidirectional converter and the full-bridge converter. As the output voltage of the proposed converter is not reversed this topology provides remarkable advantages than the other topologies when battery is used as the backup. The output voltage can be used to power the LED light which needs the input voltage not more than 50 V. The control action was implemented by using conventional controller to maintain power mismatch in the system by tracking maximum power and by regulating the battery voltage and the output voltage. The working principles of the proposed converter are also analyzed in detail. The performances of the system are also analyzed under the conditions of different insolation and load current.

**Keywords:** SEPIC/Zeta converter, Bidirectional converter, PI Control, Power mismatch, PV system

## I. Introduction

As the demand for the electric power generation increases, the generation of the power from the renewable energy sources increases drastically. Thus the electric power can be generated either by using any of the renewable energy sources. As the renewable energy sources being intermittent in nature and unpredictable, dc-dc converters along with the storage elements are required to supply the load smoothly as in case of the stand-alone system. Such that the energy storage element increases the system dynamics under less power generation on the source side.

A multi-input dc-dc converter with the common dc link [1-4] is used to interconnect all the sources and the load along with the energy storage devices. But these converters were developed by using increased number of conversion devices with complex control circuitry. The problems associated with former converter were vanished by introducing the multiport dc-dc converter [5-6]. These multi-port dc-dc converters can interface several number of renewable energy sources on the input side and loads on the output side. Thus the later converter was more advantageous as it increases the flexibility of different voltage levels with less number of the conversion devices, centralised controller and provides the quick dynamic response for the power management in the system. Multi-port topologies finds wide application in the field of remote communication system, satellite application, traffic lights, uninterrupted power supplies, electric vehicles, powering domestic applications, etc. Different topologies were associated in developing the multi-port converters [7-8] like non-isolated topology, isolated topology and partially isolated topology.

This paper focuses on the partially isolated three-port topology of which two ports are associated on the input side with one isolated output port. One of the input ports is connected to the solar photovoltaic system and the other is connected to the battery. Hence the topology of SEPIC/Zeta three-port bidirectional converter (SEPIC/ZetaTP-BDC) which is obtained by integrating the two bidirectional and the full bridge converter [9].

## II. Working Principle and the Analysis of SEPIC/Zeta TP-BDC with Operating Modes

The SEPIC/Zeta BDC consists of two switching legs with two switches in each leg connected to the source voltage. Each switching leg is capable of generating a square-wave voltage. The output can be controlled by applying the phase-shift between the voltages obtained in two switching legs, which is termed as the phase-shift full-bridge converter (PS-FBC) [10]. The square wave voltage was also obtained from the non-isolated BDC. Thus a multi-port converter was obtained by combining both the FBC and the two BDC by sharing common switching cells. SEPIC/ZetaTP-BDC converter was obtained by connecting two BDC in parallel. The PWM plus the phase shift is used to regulate the output voltage and the power balance between the ports.

The proposed SEPIC/Zeta TP-BDC is shown in Fig. 1 comprises of the two BDC's, full bridge rectifier with the diodes  $D_1 - D_4$ , inductance  $L_1-L_4$  and the capacitance  $C_b, C_1-C_2$ . The isolation transformer is used to isolate the PV source and the battery from the load. The switches  $S_1-S_4$  are connected to the transformer primary winding by means of the blocking capacitor,  $C_b$ . The SEPIC converter was achieved by the two switches  $S_1$  and  $S_2$ , the inductor  $L_1$  and  $L_4$  and the capacitor  $C_1$ . Similarly Zeta converter was achieved by the switches  $S_3$  and  $S_4$ , the inductor  $L_2$  and  $L_3$  and the capacitor  $C_2$ . The parameters of the proposed converter are given in Table I. The output voltage of both the SEPIC and the Zeta remains same which is non-inverting one but the only difference is the way by which the components are connected. The general output voltage equation  $V_o$  of the SEPIC/Zeta converter is given by

$$V_o = \frac{V_{pv} \cdot D}{(1-D)} \tag{1}$$

Where  $D$  is the duty cycle and  $V_{pv}$  is the input voltage of the converter. The Duty cycles of  $S_2$  ( $S_1$ ) and  $S_4$  ( $S_3$ ) are adopted as two control variables to control the power exchanging between PV and the battery. The phase shift between the switches  $S_2$  and  $S_4$  is  $\phi$ , the output voltage equation of the proposed converter becomes

$$V_o = nV_b \left( \frac{\phi}{\pi} (1 - \Delta D_{pv}) \right) \quad \Delta D_{pv} > 0 \quad V_o = nV_b \left( \frac{\phi}{\pi} (1 + \Delta D_{pv}) \right) \quad \Delta D_{pv} < 0 \tag{2}$$

Table I. Parameters of the three-port converter

Parameters	Values
PV voltage, $V_{pv}$	30-50V
Input power, $P_{pv}$	0-220 W
Battery voltage, $V_b$	72 V
Required output voltage, $V_o$	50 V
Output power, $P_o$	0-220 W
Turns ratio, $n$	0.833
Switching frequency, $f_s$	100 kHz
Capacitance, $C_1, C_2, C_b$	200 $\mu$ F
Inductance, $L_1, L_2, L_3, L_4$	220 $\mu$ H

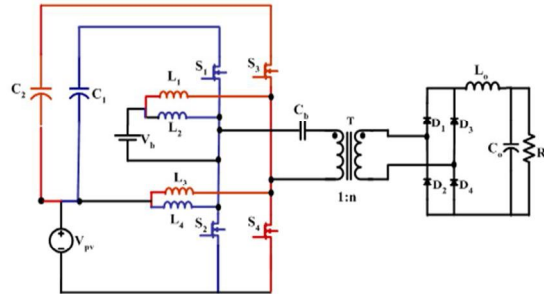


Figure 1. SEPIC/Zeta TP-BDC

The transformer turns ratio is chosen to be 1: n and its operating switching frequency is 100 kHz. In one cycle there are six switching states and the equivalent circuit diagram is shown in Fig. 2.

**State I [t<sub>0</sub>-t<sub>1</sub>]:** In this state which switches S<sub>2</sub> and S<sub>3</sub> is turned on and S<sub>1</sub> and S<sub>4</sub> is turned off. The inductors L<sub>4</sub> are charges whereas L<sub>1</sub>, L<sub>2</sub> and L<sub>3</sub> discharges [11]. The voltage applied to the primary of the transformer decreases from zero to negative. The inductor current (i<sub>L0</sub>) freewheels through the diodes D<sub>1</sub> – D<sub>4</sub> thereby short circuiting the secondary side of the transformer. The corresponding inductor current were given by the following equation.

$$\frac{dI_{L1}}{dt} = \frac{V_{pv} - V_b}{L_1} , \quad \frac{dI_{L4}}{dt} = \frac{V_{pv} - V_b}{L_4} \tag{3}$$

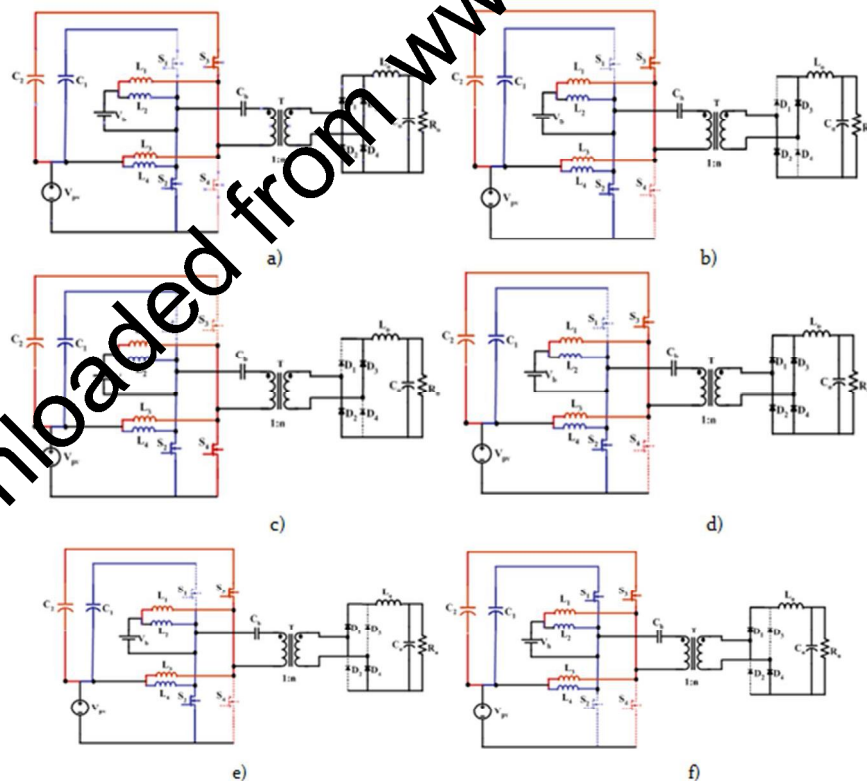


Figure 2. Equivalent circuit of the SEPIC/Zeta converter at different switching states a) t<sub>0</sub>-t<sub>1</sub> b) t<sub>1</sub>-t<sub>2</sub> c) t<sub>2</sub>-t<sub>3</sub> d) t<sub>3</sub>-t<sub>4</sub> e) t<sub>4</sub>-t<sub>5</sub> f) t<sub>5</sub>-t<sub>6</sub>

**State II [t<sub>1</sub>-t<sub>2</sub>]:** In this state the switch position remain as that of the previous state but the only difference is that the diodes D<sub>1</sub> and D<sub>4</sub> on the full bridge rectifier side are reverse biased. Therefore the the filter inductor current (i<sub>L0</sub>) flows through the diode which are forward biased. The transformer primary is supplied with the negative voltage.

**State III [t<sub>2</sub>-t<sub>3</sub>]:** At t<sub>2</sub> the switches in the upper limb S<sub>1</sub> and S<sub>3</sub> is turned off and lower limb switches S<sub>4</sub> and S<sub>2</sub> remains ON. The inductors L<sub>1</sub> and L<sub>2</sub> discharges whereas L<sub>3</sub> and L<sub>4</sub> charges. As the rectifier diodes maintain the same state, no voltage is applied to the transformer.

$$\frac{dIL_3}{dt} = \frac{V_{pv} - V_b}{L_3}, \quad \frac{dIL_4}{dt} = \frac{V_{pv} - V_b}{L_4}, \quad \frac{dIL_2}{dt} = \frac{V_{pv}}{L_2} \tag{4}$$

**State IV [t<sub>3</sub>-t<sub>4</sub>]:** In this state the switches S<sub>3</sub> and S<sub>2</sub> are in ON position and the switches S<sub>1</sub> and S<sub>4</sub> are in OFF position. The inductors L<sub>1</sub>, L<sub>2</sub> and L<sub>3</sub> charges and inductor L<sub>4</sub> discharges. The transformer voltage gradually rises from zero to positive. The inductor current (i<sub>L0</sub>) freewheels through the diodes D<sub>1</sub> and D<sub>4</sub>.

$$L_3 \frac{dIL_3}{dt} + V_{pv} = L_1 \frac{dIL_1}{dt} + V_b \tag{5}$$

**State V [t<sub>4</sub>-t<sub>5</sub>]:** The inductor positions are just complementary to that of the state III as the switches S<sub>3</sub> and S<sub>2</sub> are turned on and the switches S<sub>1</sub> and S<sub>4</sub> are turned OFF. Voltage applied to the transformer primary winding is positive.. The current (i<sub>L0</sub>) fully flows only through other two diodes D<sub>1</sub> and D<sub>4</sub>.

**State VI [t<sub>5</sub>-t<sub>6</sub>]:** In this state the switches S<sub>4</sub> and S<sub>2</sub> is turned OFF and the switches S<sub>3</sub> and S<sub>1</sub> are in ON state. In this state the voltage applied to the primary is zero. The current (i<sub>L0</sub>) fully flows only through D<sub>1</sub> and D<sub>4</sub>.

The simulated corresponding key waveforms of the proposed SEPIC/Zeta TP-BDC converter in which the two switches in each leg are complementary to each other are shown in Fig. 3.

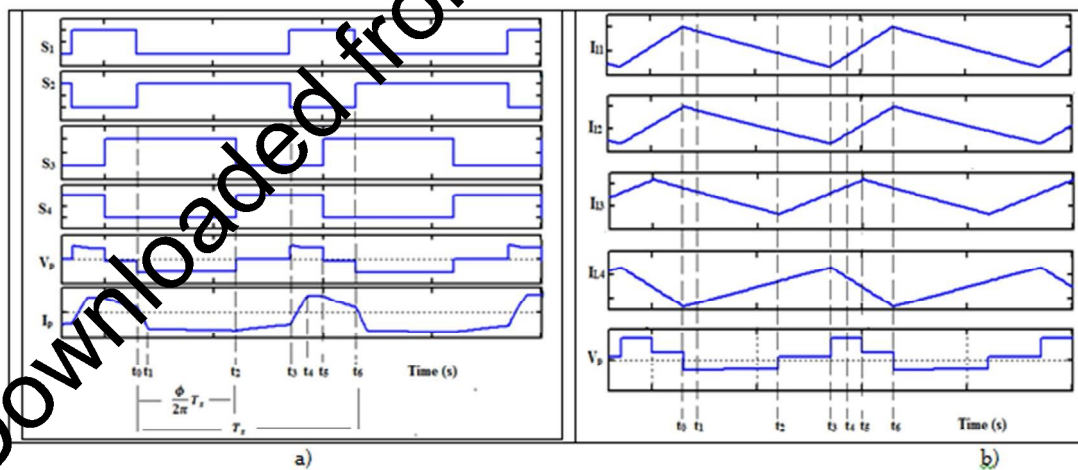


Figure 3. Key waveforms of SEPIC/Zeta TP-BDC a) Generated pulse b) Characteristics of the inductor at different switching states

### Operating modes of the proposed converter for hybrid sources

In a standalone system, the power mismatch can be met by three ways of power flow. Thus the flow of power can be from 1) PV to load 2) PV to battery and 3) Battery to load. As the proposed topology consists of three ports, the two ports are controlled independently and the third is meant for the power balance. Depending upon the power flow between the ports there are three types of modes of operation like dual output mode, dual input mode and single input single output mode and the corresponding schematic diagram is shown in Fig. 4.

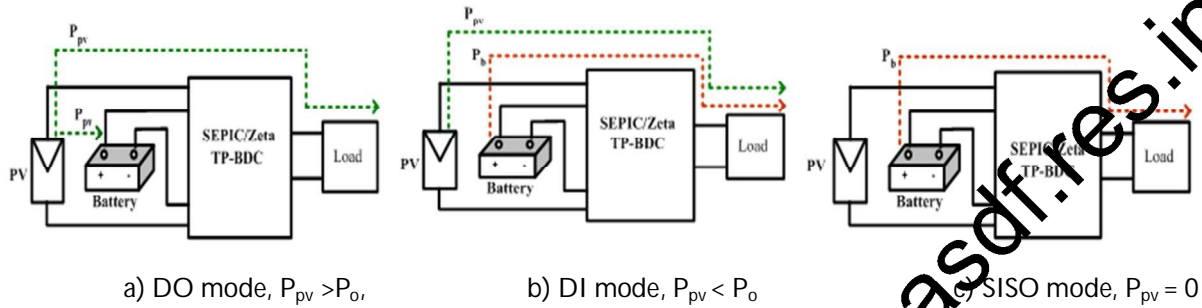


Figure 4. Operating modes of SEPIC/Zeta TP-BDC

The power flows in the input source, battery and the load port are represented as  $P_{pv}$ ,  $P_b$  and  $P_o$  respectively. Ignoring losses in the system the power balance equation is given by  $P_{pv} + P_b = P_o$  (6)

### III. Control Structure for Pulse Width Modulation and PV System

The schematic of the control structure of the integrated SEPIC/Zeta TP-BDC is shown in Fig. 5 a) for the PV-battery hybrid power system [12]. The duty cycle of the SEPIC/Zeta converter are employed to keep the power balance between the PV and the battery. With the PWM plus phase-angle-shift scheme, two of the three ports are regulated and the phase angle is used to regulate the output voltage simultaneously. Power balance in the system is achieved with three PI regulators, which were used to regulate the output voltage by achieving control of input source and by the control of the battery. To provide the required output voltage and the current, the PV source is designed in such a way that the three panels with the rating of  $I_{max} = 2.25$  A and  $V_{max} = 16.54$  V and with  $P_{max} = 37.08$  W at  $G = 1000$  W/m<sup>2</sup> and  $T = 25^\circ$ C [13] are connected in series to provide the required input voltage of 50 V and the similar two panels are connected in parallel to provide the current of 4.5 A such that the required array size becomes 3 X 2. The corresponding characteristic curves of the different array size were shown in the Fig. 5 b).

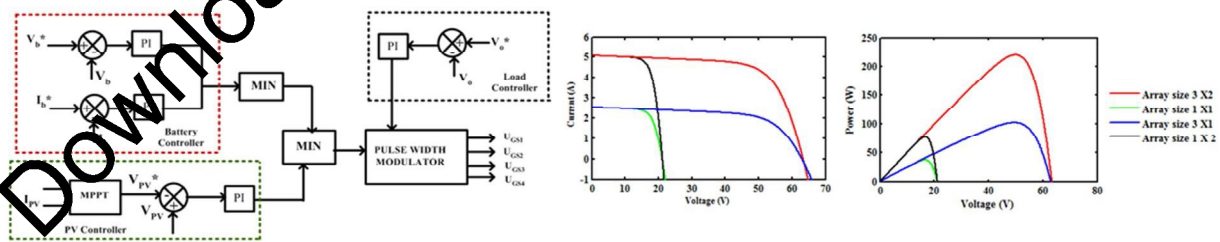


Figure 5. a) Control structure of TP-SEPIC/Zeta BDC b) Characteristic of PV system with different array size

### IV. Results and Discussion

When the power available on the input side is more than the required load, it supplies power to the load at the same time it charges the storage device. Similarly when the required load power is more than the available input power, the power stored in the storage device along with the input source supplies the load. Such that power mismatch is balanced in the system. The proposed system is designed in such a way that the PV source supplies the power of about 220 W at 1000 W/m<sup>2</sup> with the corresponding voltage and current waveforms are shown in Fig. 6.

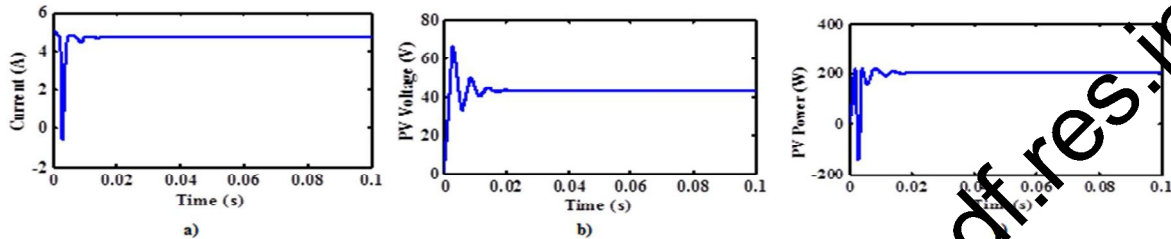


Figure 6. Performance waveforms of the PV system at the insolation of 1000 W/m<sup>2</sup> (a) PV voltage (b) PV current (c) PV Power.

The battery is designed for the 50% SOC with Rated Capacity of 40 Ah for the nominal Voltage of 72 V. As the load is designed for the 100 W to provide the required voltage of 50 V and the current of 2.5 A and its corresponding waveforms are validated in Fig. 7.

The controller is used to analyse the performance of the system under variations in the input voltage and the load current when reference value is set to as 50 V. Performance of the system was analysed by giving step change in input from high to low insolation i.e. from 1000 W/m<sup>2</sup> to 400 W/m<sup>2</sup> at 0.12 s the desired output voltage is obtained. When the insolation is 400 W/m<sup>2</sup> the system operates in the DO mode, as the insolation reduces to 400 W/m<sup>2</sup> the mode of operation changes to DI mode. When the required output power changes its value from 100 W to 200 W i.e. by providing step load change from 25 Ω to 12.5 Ω at 0.12 s at constant insolation of 1000 W/m<sup>2</sup> the required output voltage is also obtained.

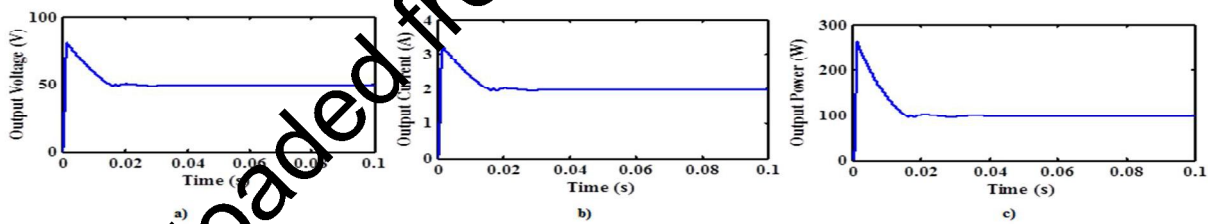


Figure 7. Performance waveforms at the port 3 (a) output voltage (b) output current (c) output power

The efficiency of the system is also analysed under different load power and it is around 94.82 % under fully loaded condition. The corresponding waveforms and results are validated in Fig. 8.

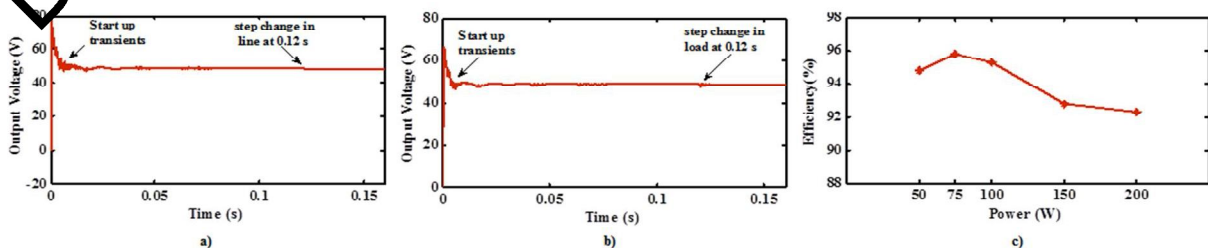


Figure 8. Output response under a) line regulation b) load regulation c) performance of PV to load

## V. Conclusion

The performance of the most effective and unique SEPIC/Zeta TP-BDC with the centralised controller was presented. The three-ports were interfaced to the solar PV system, battery and the load. The equivalent circuit at different switching states was also analysed and the corresponding equation were derived. The converter was able to balance the power mismatch between different ports at different operating conditions. The system also remains stable for various loads current and the input voltage. In future the ZVS can also be achieved for the system.

## References

1. Lalit Kumaland Shailendra Jain, "Multiple-input dc/dc converter topology for hybrid energy system," *IET Power Electronics*, vol. 6, no. 8, pp. 1483–1501, March 2013.
2. Alireza Khaligh, Jian Cao, and Young-Joo Lee, "A multiple-input dc–dc converter topology", *IEEE Transactions on Power Electronics*, vol. 24, no. 3, pp.862 – 868, March 2009.
3. A. Kwasinski and P.T Krein, "Multiple-input dc-dc converters to enhance local availability in grids using distributed generation resources," *IEEE Trans. Applied Power Electronics Conference, APEC*, pp. 1657- 1663, 2007 [22<sup>nd</sup> Annual Conference of IEEE 2007].
4. Haimin Tao, Jorge L. Duarte and Marcel A.M. Hendrix, "Multiport converters for hybrid power sources," *Power Electronics Specialists Conference, IEEE*, pp. 3412 – 3418, 2008.
5. S.H. Choung and A. Kwasinski, "Multiple-input dc-dc converter topologies comparison," *IEEE Trans. Industrial Electronics, IECON*, pp 2359-2364, 2008. [34<sup>th</sup> Annual Conference of IEEE 2008].
6. Wei Jiang and Babak Fahimi, "Multiport power electronic interface—concept, modeling and design," *IEEE Trans. on Power Electronics*, vol. 26, no. 7, pp. 1890-1900, July 2011.
7. Zhijun Qian, Osama Abdel-Rahman and Issa Batarseh, "An integrated four-port dc/dc converter for renewable energy applications," *IEEE Trans. on Power Electronics*, vol. 25, no. 7, pp. 1877-1887, July 2010.
8. Alexis Kwasinski, "Identification of feasible topologies for multiple-input dc–dc converters," *IEEE Trans. on Power Electronics*, vol. 24, no. 3, March 2009
9. Hongfei Wu, Peng Xu, Haibing Hu, Zihu Zhou and Yan Xing, "Multiport converters based on integration of full bridge and bidirectional dc-dc topologies for renewable generation system," *IEEE Trans. Industrial Electronics*, vol.61, no. 2, pp.856-869, Feb. 2014.
10. Ali Asghar Ghadimi, Hassan Rastegar and Ali Keyhani, "Development of average model for control of a full bridge PWM dc-dc converter," *Journal of Iranian Association of Electrical and Electronics Engineers*, vol. 4, no. 2, pp. 52-59, 2007.
11. Hongfei Wu, Runruo Chen, Haibing Hu and Yan Xing, " Full bridge three-port converters with wide input voltage range for renewable power system," *IEEE Trans. Power Electronics*, vol. 27, no. 9, pp. 3965-3974, Sep. 2012
12. F. Najabatkhah, S. Danyali, S. H. Hosseini, M. Sabahi and S.M. Niapour, "Modeling and control of a new three-input dc–dc boost converter for hybrid PV/FC/battery power system," *IEEE Trans. Power Electronics*, vol. 27, no. 5, pp. 2309-2324, 2012.
13. Anmed Koran, Thomas LaBella and Jih-Sheng Lai, "High efficiency photovoltaic source simulator with fast response time for solar power conditioning systems evaluation," *IEEE Trans. on Power Electronics*, vol. 29, no. 3, pp. 1285 – 1297, March 2014
14. www.mathworks.com.